



Published in final edited form as:

Inhal Toxicol. 2011 December ; 23(14): 927–937. doi:10.3109/08958378.2011.625995.

Mechanisms of crystalline silica-induced pulmonary toxicity revealed by global gene expression profiling

Rajendran Sellamuthu¹, Christina Umbricht¹, Shengqiao Li², Michael Kashon², and Pius Joseph¹

¹Toxicology and Molecular Biology Branch, Health Effects Laboratory Division, National Institute for Occupational Safety and Health (NIOSH), Morgantown, WV, USA

²Biostatistics and Epidemiology Branch, Health Effects Laboratory Division, National Institute for Occupational Safety and Health (NIOSH), Morgantown, WV, USA

Abstract

A proper understanding of the mechanisms underlying crystalline silica-induced pulmonary toxicity has implications in the management and potential prevention of the adverse health effects associated with silica exposure including silicosis, cancer and several auto-immune diseases. Human lung type II epithelial cells and rat lungs exposed to crystalline silica were employed as experimental models to determine global gene expression changes in order to understand the molecular mechanisms underlying silica-induced pulmonary toxicity. The differential gene expression profile induced by silica correlated with its toxicity in the A549 cells. The biological processes perturbed by silica exposure in the A549 cells and rat lungs, as identified by the bioinformatics analysis of the differentially expressed genes, demonstrated significant similarity. Functional categorization of the differentially expressed genes identified cancer, cellular movement, cellular growth and proliferation, cell death, inflammatory response, cell cycle, cellular development, and genetic disorder as top ranking biological functions perturbed by silica exposure in A549 cells and rat lungs. Results of our study, in addition to confirming several previously identified molecular targets and mechanisms involved in silica toxicity, identified novel molecular targets and mechanisms potentially involved in silica-induced pulmonary toxicity. Further investigations, including those focused on the novel molecular targets and mechanisms identified in the current study may result in better management and, possibly, reduction and/or prevention of the potential adverse health effects associated with crystalline silica exposure.

Keywords

Crystalline silica; pulmonary toxicity; gene expression profile; mechanisms

Address for Correspondence: Pius Joseph, MS 3014, Toxicology and Molecular Biology Branch, National Institute for Occupational Safety and Health (NIOSH), 1095 Willowdale Road, Morgantown, WV 26505, USA. Tel: (304)285-6240. Fax: (304)285-5708. pcj5@cdc.gov.

Declaration of interest

The authors report no declaration of interest.

Introduction

Millions of workers worldwide are occupationally exposed to crystalline silica at concentrations that are sufficient to cause serious health effects. In addition to silicosis, a life-threatening lung pneumoconiosis, crystalline silica exposure is associated with the development of several diseases such as bronchitis, emphysema, tuberculosis, systemic sclerosis, rheumatoid arthritis, lupus, and chronic renal disease (Cooper et al., 2002). The International Agency for Research on Cancer (IARC), on the basis of increasing evidence obtained from epidemiological and laboratory animal studies, has classified crystalline silica as a carcinogen (IARC, 1997). In spite of increasing evidence for the involvement of crystalline silica in various diseases, the underlying mechanisms for its toxicity, especially at the molecular level, are not fully understood. Many of the adverse pulmonary effects of crystalline silica exposure have been attributed to the induction of inflammation, the single most investigated and important biological response associated with exposure to silica (Castranova et al., 2002; Porter et al., 2002; Hamilton et al., 2008). However, it is not clear whether inflammation alone accounts for the multiple pathological conditions resulting from occupational exposure to crystalline silica. A better understanding of all possible molecular targets and mechanisms underlying the various pathological conditions of silica is, therefore, essential to manage, as well as to prevent, the potential adverse health effects associated with crystalline silica exposure.

Advances in high throughput gene expression profiling, such as microarray analysis, enable a comprehensive understanding of the effects of toxic agents in biological systems. Identification of the genes that are differentially expressed in response to exposure to a toxic agent and careful analysis of the differentially expressed genes by employing appropriate statistical and computational approaches may provide valuable information regarding the molecular mechanism(s) underlying the toxicity of the agent. The gene expression data, in addition, may be used to generate novel hypotheses regarding the molecular mechanisms underlying the toxicity of the agent being investigated. The differentially expressed genes and/or their products, following appropriate validation, may be employed as biomarker(s) for exposure as well as toxicity of the agent under investigation. In the past, microarray-based transcriptomics studies have been successfully employed to gain insights into the molecular mechanisms underlying the toxicity of chemicals (Waring et al., 2001; Hamadeh et al., 2002) as well as to identify molecular markers for their toxicities (Amin et al., 2004; Fielden et al., 2008). Although these techniques exist, microarray-based transcriptomics studies have been employed only sparingly to investigate the molecular mechanisms of crystalline silica – an agent that has been historically known to result in serious adverse health effects in human. The objective of the present study, therefore, was to identify potential molecular targets and/or mechanisms underlying silica-induced pulmonary toxicity.

Presently, human lung epithelial cells, A549, were used as an *in vitro* model to gain insights into the molecular mechanisms underlying crystalline silica-induced pulmonary toxicity. The silica-induced cytotoxicity and differential gene expression profile correlated well with its toxicity in A549 cells. Functional categorization of the differentially expressed genes identified cancer, cellular movement, cellular growth and proliferation, cell death,

inflammatory response, cell cycle, cellular development, and genetic disorder as the top ranking biological functions perturbed in the A549 cells in response to silica exposure and the resulting toxicity. Cellular processes perturbed by silica exposure, as evidenced from the results of the bioinformatics analysis of differentially expressed genes in A549 cells, were further confirmed by the results of global gene expression profiling in the lungs of rats exposed by inhalation to a toxic concentration of respirable crystalline silica particles. Taken together, the findings of our *in vitro* and *in vivo* toxicity and gene expression studies provided insights, including novel ones, into the molecular targets and mechanisms underlying the pulmonary toxicity of crystalline silica.

Materials and methods

Cell culture and silica cytotoxicity determination

Mycoplasma-free human lung epithelial cells, A549 (Catalogue number CCL-185, ATCC, Manassas, VA), were cultured under standard cell culture conditions in F-12K medium containing 10% bovine fetal serum and penicillin and streptomycin as antibiotics. Endotoxin-free Min-U-Sil-5 crystalline silica (US Silica, Berkeley Springs, WV) was sieved through a 10 µm mesh filter (Thomas Scientific, Swedesboro, NJ) for 20 minutes and used immediately to treat the cells. The filtered silica particles were resuspended in serum-free cell culture medium to achieve the desired final concentrations. The dose-response of silica exposure was determined by treating exponentially growing A549 cells in the individual wells of a 6-well cell culture dish (1.5×10^5 cells/well) with the filtered silica particles at final concentrations of 15, 30, 60, 120, and 240 µg/cm² of cultured area for 6-hours. For the time-course study, the cells were treated with filtered silica at a final concentration of 60 µg/cm² of cultured area for 2-, 6-, and 24-hours. The experiment was repeated five times for each silica concentration and exposure period. At the end of the silica exposure, cytotoxicity was determined by assaying the activity of lactate dehydrogenase (LDH) in the cell culture medium by employing the LDH Assay Kit (Roche Diagnostics, Indianapolis, IN) following the protocol provided by the manufacturer. Simultaneously, the control and silica exposed cells were collected for RNA isolation.

Lung samples of silica exposed rats

The lung samples used in this study were obtained from rats which were used in one of our previous studies (Sellamuthu et al., 2011). The rat experiment was conducted by following a protocol that was approved by the Institutional Animal Care and Use Committee (ACUC), National Institute for Occupational Safety and Health (NIOSH), Morgantown, WV. Stated briefly, approximately 3-months old CDF strain male Fisher 344 rats (Charles River Laboratories, Wilmington, MA) were exposed to Min-U-Sil-5 crystalline silica by inhalation at a concentration of 15 mg/m³, 6 hours/day, for 5 consecutive days. At 16-hours following termination of the 5th day of silica exposure, the control (exposed to filtered air) and silica exposed rats were sacrificed and pulmonary toxicity was determined (Sellamuthu et al., 2011). The upper lobe of the right lung was immediately transferred to RNA later (Ambion, Inc, Austin, TX) and stored at -80°C until RNA isolation.

RNA isolation

Total RNA, free of contaminating DNA and proteins, was isolated from the control and silica exposed A549 cells using the RNeasy Kit (Qiagen, Inc, Valencia, CA). Total RNA was isolated from rat lung samples using RNeasy Fibrous Tissue Mini Kit (Qiagen, Inc.). Briefly, 20–30 mg lung tissue were homogenized in Buffer RLT containing β -mercaptoethanol and two 2.4 mm Zirconia Beads (BioSpec Products Inc, Bartlesville, OK) using a Mini beadbeater-8 (BioSpec Products Inc.) for 20 seconds. After centrifugation at 10,000g for 3 minutes at room temperature, the supernatant containing the RNA was applied to the RNeasy column and processed as directed in the RNeasy Fibrous Tissue Mini Kit protocol. The integrity of the RNA samples was determined using the Agilent 2100 Bioanalyzer (Agilent Technologies, Palo Alto, CA) and quantitated by UV spectrophotometry. Only RNA samples that exhibited an RNA integrity number (RIN) >8.0 were used in the gene expression analysis.

Microarray analysis of global gene expression profile

The RNA isolated from the A549 cells and the rat lung samples was analyzed for global gene expression profile using Human HT-12_v3_Beadchip and RatRef-12 V1.0 Expression BeadChip arrays (Illumina, Inc, San Diego, CA), respectively. All microarray experiments were performed to comply with Minimal Information About a Microarray Experiment (MIAME) protocols. Biotin-labeled cRNA was generated from 375 ng total RNA samples each by employing the Illumina Totalprep RNA Amplification Kit (Ambion, Inc.). Chip hybridizations, washing, Cy3-streptavidin staining, and scanning of the chips on the Beadstation 500 platform (Illumina, Inc.) were performed following the protocols provided by the manufacturer.

Metrics files from the bead scanner were checked to ensure that all samples fluoresced at comparable levels before samples were loaded into Beadstudio (Framework version 3.0.19.0) Gene Expression module v.3.0.14. Housekeeping, hybridization control, stringency, and negative control genes were checked for proper chip detection. BeadArray expression data were then exported with mean fluorescent intensity across like beads and bead variance estimates into flat files for subsequent analysis.

Illumina BeadArray expression data was analyzed in Bioconductor using the 'lumi' and 'limma' packages. Bioconductor is a project for the analysis and comprehension of genomic data and operates in R, a statistical computing environment (Ihaka and Gentleman, 1996). The 'lumi' Bioconductor package was specifically developed to process Illumina microarrays and covers data input, quality control, variance stabilization, normalization, and gene annotation (Gentleman et al., 2004). Normalized data were then analyzed using the 'limma' package in R. In short, limma fits a linear model for each gene, generates group means of expression, and calculates p values and log fold changes which are converted to standard fold changes. The raw p values were corrected for false discovery rate (FDR) using the Benjamini and Hochberg procedure (Benjamini and Hochberg, 1995). Only genes with FDR p value <0.05 compared with the controls were considered as significantly differentially expressed and used as input for subsequent bioinformatics analysis.

The normalized microarray data was further analyzed using USFDA's ArrayTrack system (Tong et al., 2004). The initial genomic analysis used the methodology of the Gene Ontology (GO) consortium available within the ArrayTrack. Subsequent bioinformatics analysis was conducted using the Ingenuity Pathway Analysis (IPA, Ingenuity Systems, www.ingenuity.com). IPA software is designed to map the biological relationship of the uploaded genes and classify them into categories according to published literature in the database. The criteria required for a biological process to be considered significantly enriched in response to silica exposure and toxicity was that the process within a gene set was represented with a significance level for enrichment of $p < 0.05$. The biological processes significantly enriched ($p < 0.05$) but represented by fewer than 10 genes were filtered out to identify the biological processes most robustly perturbed by crystalline silica exposure in the A549 cells and rat lungs.

Quantitative real-time polymerase chain reaction (QRT-PCR) analysis

The objective of the QRT-PCR analysis was to confirm the microarray data. For this purpose, a representative set of seven genes that exhibited a significant (FDR $p < 0.05$) and silica concentration-dependent overexpression at all concentrations of silica employed in the A549 cells was selected. The nucleotide sequences of the primers used in the QRT-PCR analysis of the selected genes and the housekeeping gene, *human β -2-microglobulin (HB2M)*, are presented in Table 1. The PCR amplification, detection of the PCR amplified gene products, and their quantitations were performed with a 7900 HT Fast Real-time PCR machine and the SYBR Green PCR MasterMix (Applied Biosystems, Foster City, CA). The expression levels of the genes were normalized to that of the housekeeping gene and the fold changes in expression compared with the controls were calculated using the formula $2^{-(Ct_{\text{target}} - Ct_{\text{HB2M}})}$.

Statistical analysis of data

Nonmicroarray data between the control and silica exposed groups were compared using the one way ANOVA test. *Post hoc* comparisons were made with Fisher's least significant difference (LSD) test. A p value of <0.05 was considered statistically significant.

Results

Silica exposure resulted in cytotoxicity and differential gene expression profile in A549 cells

Exposure to crystalline silica resulted in a concentration- and time-dependent cytotoxicity and differential gene expression profile in the A549 cells (Figure 1A–D). The silica-induced cytotoxicity and the number of differentially expressed genes in the cells exhibited correlation coefficients (r^2 values) of 0.89 and 0.98, respectively, for the dose-response and time-course study.

QRT-PCR analysis

QRT-PCR analysis results confirmed the concentration-dependent trend of overexpression of all seven selected genes in the silica exposed cells compared to the control (Figure 2). In general, the magnitude of gene expression changes measured by QRT-PCR was greater than

that measured by microarray analysis. This may be attributed to the lower dynamic range afforded by microarray analysis compared with the QRT-PCR analysis.

Bioinformatics analysis of gene expression data

Bioinformatics analysis of the differentially expressed genes by GO and IPA identified several biological processes/functions that were significantly affected in the A549 cells and rat lungs in response to crystalline silica exposure. The top eight ranking biological functions identified by IPA that were significantly affected by silica exposure in the A549 cells were cancer, cellular movement, cellular growth and proliferation, cell death, inflammatory response, cell cycle, cellular development, and genetic disorder (Table 2). It is important to note that all of the top ranking biological functions exhibited a concentration- and time-dependent response to silica exposure in the A549 cells (Figure 3A and B, respectively) as was noticed in the case of silica-induced cytotoxicity and differential gene expression profile (Figure 1A–D). All of the top eight ranked biological functions identified in the silica exposed A549 cells were also found significantly affected in the lungs of silica exposed rats (Table 2). It is worth mentioning that with the exception of cell cycle, all other top eight ranked biological functions that were perturbed by silica exposure in the A549 cells were also ranked within top 15 in the lungs of the silica exposed rats (Table 2). Similar to the findings of IPA, a significant similarity was noticed between the A549 cells and rat lungs with respect to the biological processes perturbed by silica exposure as evidenced from the results of GO analysis (data not presented). A selected list of genes that are found significantly differentially expressed in the silica exposed A549 cells and belong to important IPA and GO biological processes/functions categories that might be of relevance to the pulmonary effects of silica exposure are presented in Table 3 and the functional significance of their differential expression with respect to the pulmonary effects of silica exposure is discussed in the Discussion section.

Discussion

Recent developments in transcriptomics research have facilitated a better understanding of the potential for chemicals to cause toxicity as well as the molecular mechanisms underlying chemical toxicity. Lungs have been identified as the primary target organ for silica toxicity in laboratory animals as well as in human. A549 cells, the *in vitro* model employed in the present study, are type II epithelial cells derived from human lungs and have been previously used as a relevant model to study the pulmonary toxicity of chemicals (Thompson and Burcham, 2008) and particulate materials, including silica (Stringer and Kobzik, 1998; Øverick et al., 2004). Exposure of A549 cells to crystalline silica resulted in cytotoxicity and differential gene expression profile, and these were dependent on the concentration and duration of silica exposure (Figure 1A–D). The temporal relationship between cytotoxicity and differential gene expression profile observed in the A549 cells in response to their exposure to silica suggested the potential use of the gene expression data to study the mechanisms underlying silica toxicity. Gene expression data obtained from the lungs of rats exposed to a toxic concentration of silica particles provided additional credence to the gene expression data obtained from the A549 cells. Significant pulmonary toxicity was noticed in the rats in response to silica exposure (Sellamuthu et al., 2011) and the results

of the microarray analysis demonstrated that the silica-induced pulmonary toxicity in the rats was associated with significant differential expression of 2904 genes (data not presented).

Bioinformatics analysis of the differentially expressed genes in the silica exposed A549 cells and rat lungs exhibited a remarkable similarity with respect to the biological functions/processes that were affected in response to silica exposure and the resulting toxicity (Table 2). This suggests the potential involvement of common toxicity mechanisms in the *in vitro* and *in vivo* models employed in the current study irrespective of the inherent differences between the A549 cells (a carcinoma cell line) and rat lungs consisting of heterogeneous population of cells. In addition, the top ranking IPA biological functions identified as being affected by silica exposure in the two models were dependent on the concentration and duration of silica exposure in the A549 cells (Figures 3A and B).

The finding that silicotic lungs are in a state of oxidative stress (Vallyathan and Shi, 1997) has led to the belief that oxidant-mediated lung damage may participate in the development of silica-induced pulmonary diseases. Many of the genes which were found differentially expressed in the A549 cells in response to silica exposure, in addition to supporting the generation of ROS, provided insights into the cellular mechanisms underlying silica-induced oxidative stress and the resulting pulmonary damage. In agreement with previous reports, the significant and silica concentration-dependent overexpression of oxidative stress-responsive genes such as *fos* and *jun* (Ding et al., 2001) and members of the *NFκB* family (Castranova, 2004) of genes noticed presently suggested the generation of ROS and resulting oxidative stress in the silica exposed cells. Superoxide anion, a reactive oxygen species generated in response to silica exposure, undergoes dismutation catalyzed by superoxide dismutase (SOD) to generate hydrogen peroxide (H_2O_2). A significant amount of H_2O_2 is also generated during the metabolism of spermine catalyzed by spermine oxidase (SMOX) (Murray-Stewart et al., 2008). The toxic and reactive H_2O_2 thus generated is subsequently detoxified, predominantly by catalase, in order to prevent its interaction with intracellular target(s) potentially leading to toxicity. The net result of the significant and silica concentration-dependent overexpression of *SOD* and *SMOX* with simultaneous decrease in the expression of *catalase*, as noticed in the silica exposed A549 cells, is the cellular accumulation of toxic and reactive H_2O_2 which might account, at least in part, for the silica-induced oxidative stress and cytotoxicity that was noticed in the A549 cells. *NFκB* is an oxidative stress-responsive transcription factor that controls the expression of a variety of chemokines, cytokines, adhesion molecules and growth factors (Chen et al., 1999a) that are involved in the induction of chronic inflammation (Barnes and Karin, 1997). AP-1, consisting of homo- and hetero-dimers of *fos* and *jun*, is also an oxidative stress-responsive transcription factor that regulates the expression of a large number of genes involved in carcinogenesis and inflammation (Mossman et al., 1997; Robledo and Mossman, 1999).

Crystalline silica particles, following their entry into the respiratory system, are engulfed by alveolar macrophages (AMs) for their detoxification. The interaction between silica particles and AM may result in a cascade of cellular events including the activation of transcription factors and the release of ROS, reactive nitrogen species (RNS), chemotactic factors, lytic enzymes, cytokines, and growth factors. The net result is the activation of AMs culminating

in their death and the release of silica particles within the lungs. Apoptosis plays a major role in silica-induced death of AMs and many of the resulting pulmonary effects of silica particles. The bioinformatics analysis of the gene expression data in the silica exposed A549 cells and rat lungs, in addition to supporting the involvement of apoptosis in silica-induced pulmonary toxicity, provided novel insights into the mechanisms potentially underlying silica-induced apoptosis. The ability of silica to interact with DNA and, therefore, to result in DNA damage has been previously demonstrated (Mao et al., 1994). Even though it has been fairly well-established that silica exposure results in apoptosis indirectly through the generation of ROS (Santarelli et al., 2004; Hu et al., 2006), the apoptotic implication of direct DNA damage induced by silica, if any, is not known. *Growth arrest and DNA damage-inducible (GADD)* genes are a family of genes that are found significantly overexpressed in cells undergoing apoptosis (Hollander et al., 1997). The GADD proteins interact with a diverse array of proteins to facilitate apoptosis. For example, *GADD45 α* , a *p53*-regulated gene, interacts with other *p53*-regulated genes that play an important role in apoptosis (Sarkar et al., 2002). The significant and silica concentration-dependent overexpression of *GADD34* and *GADD45 α* — two important members of the *GADD* family of genes, noticed in the silica exposed A549 cells (Table 3) is a novel finding. It is worth investigating the involvement, if any, of the GADD family of genes in silica-induced apoptosis as well as the mechanisms potentially involved in the process. Early growth response 1 (*EGR1*) is a transcription factor that plays a prominent role in apoptosis through its interaction with the *p53* family of genes (Yu et al., 2007). The very high and silica concentration-dependent overexpression of *EGR1* noticed in the A549 cells (Table 3 and Figure 2) also warrants future investigations addressing the mechanisms underlying silica-induced overexpression of *EGR1* and its potential involvement in silica-induced apoptosis.

Silica exposure results in the induction of inflammation (Chen et al., 1999b; Fubini and Hubbard, 2003; Porter et al., 2004), and a definite role for inflammation in many of the toxic effects of silica has been demonstrated (Castranova et al., 2002; Porter et al., 2002). Induction of pulmonary inflammation, as evidenced from a significant increase in the number of AMs and PMNs as well as the activities of pro-inflammatory cytokines, MCP1 and MIP-2, was noticed in the rat lung tissue samples which were used in the current study to determine gene expression profile by microarray analysis (Sellamuthu et al., 2011). Bioinformatics analysis of the gene expression profile of the silica exposed A549 cells and rat lungs, in addition to supporting the involvement of inflammation in the pulmonary effects of silica, provided insights into the molecular mechanisms underlying silica-induced inflammation. Transcripts for several genes involved in inflammation were significantly differentially expressed in the A549 cells and rat lungs in response to silica exposure and toxicity. Among the functional categories of genes whose expressions were significantly affected by silica exposure in the A549 cells and rat lungs, inflammatory response ranked five and seven, respectively (Table 2).

The present study also provided many novel insights with respect to the potential cellular target(s) and/or the molecular mechanisms underlying the pulmonary toxicity of crystalline silica. The Kruppel-like family (KLF) of transcription factors are known for their involvement in cellular proliferation and cancer (Ghaleb and Yang, 2008; Mori et al., 2009;

Nakamura et al., 2009). Several of the *KLFs* were significantly overexpressed in the A549 cells in response to their exposure to crystalline silica (Table 3). To the best of our knowledge, the role of *KLFs*, if any, in the carcinogenic effect of crystalline silica has not been investigated so far. Therefore, determining the functional consequences of the overexpression of the *KLF* genes in the silica exposed cells may provide a better understanding of the molecular mechanisms underlying silica-induced cancer. As discussed above, investigating the functional implication(s) of the significant overexpression of *GADD34* and *GADD45a* noticed in the silica exposed A549 cells may provide novel insights into the molecular mechanisms underlying silica-induced DNA damage and apoptosis. Other examples for the novel findings of the current study that may require further attention include the significant overexpression of genes such as *OKL-38* and *GDF-15* noticed in the silica exposed cells (Table 3). *OKL-38* is an oxidative stress-responsive gene and plays an important role in apoptosis (Li et al., 2007). *GDF-15* is a member of the TGF super family of genes and is known for its involvement in apoptotic and inflammatory pathways during tissue injury (Schlittenhardt et al., 2004). Dual specificity phosphatases (DUSPs) are a family of genes that are overexpressed in cells in response to stress, including oxidative stress (Lang et al., 2006). A definite role for the various members of DUSP in cellular signal transduction processes involved in apoptosis, proliferation, cancer, and innate and adaptive inflammation has been reported (Camps et al., 2000; Lang et al., 2006). This is attributed, mainly, to the role of DUSPs on their substrates, mitogen activated protein kinases (MAPKs), which are key components of the signal transduction process controlling vital cellular processes (Camps et al., 2000). A definite role for MAPKs in the pulmonary toxicity induced by silica has been established (Fubini and Hubbard, 2003). The significant and silica concentration-dependent overexpression of *DUSP1* and *DUSP5* noticed in the A549 cells (Table 3 and Figure 2A and B) may suggest their involvement, by yet to be identified mechanisms, in the pulmonary toxicity of crystalline silica.

In summary, a remarkable similarity was noticed between the molecular responses of the silica exposed A549 cells and the rat lungs, the two models employed in the current study. In addition to confirming many of the previously established mechanisms underlying the pulmonary response to silica exposure, the current study involving transcriptomics analysis provided novel insights regarding the molecular targets and mechanisms potentially involved in silica-induced pulmonary toxicity. Further investigations, especially those focused on the novel molecular targets and mechanisms identified in the current study, may provide a better understanding of the mechanisms underlying the various pathological conditions associated with silica exposure. This, in turn, may result in better management and, possibly, reduction and/or prevention of the potential adverse health effects associated with crystalline silica exposure.

Supplementary Material

Refer to Web version on PubMed Central for supplementary material.

Acknowledgements

The authors thank Bean Chen, Amy Cumpston, Jared Cumpston, David Frazer, Howard Leonard, and Walter McKinney (NIOSH, Morgantown, WV) for assistance with inhalation exposure of rats to crystalline silica. The findings and conclusions in this report are those of the authors and do not necessarily represent the views of NIOSH. The microarray data have been deposited in the Gene Expression Omnibus Database, <http://www.ncbi.nlm.nih.gov/geo> (accession number GSE30216).

References

- Amin RP, Vickers AE, Sistare F, Thompson KL, Roman RJ, Lawton M, Kramer J, Hamadeh HK, Collins J, Grissom S, Bennett L, Tucker CJ, Wild S, Kind C, Oreffo V, Davis JW 2nd, Curtiss S, Naciff JM, Cunningham M, Tennant R, Stevens J, Car B, Bertram TA, Afshari CA. Identification of putative gene based markers of renal toxicity. *Environ Health Perspect.* 2004; 112:465–479. [PubMed: 15033597]
- Barnes PJ, Karin M. Nuclear factor- κ B: A pivotal transcription factor in chronic inflammatory diseases. *N Engl J Med.* 1997; 336:1066–1071. [PubMed: 9091804]
- Benjamini Y, Hochberg Y. Controlling the false discovery rate: A practical and powerful approach to multiple testing. *J R Stat Soc Ser.* 1995; 57:289–300.
- Camps M, Nichols A, Arkinstall S. Dual specificity phosphatases: A gene family for control of MAP kinase function. *FASEB J.* 2000; 14:6–16. [PubMed: 10627275]
- Castranova V, Porter D, Millecchia L, Ma JY, Hubbs AF, Teass A. Effect of inhaled crystalline silica in a rat model: Time course of pulmonary reactions. *Mol Cell Biochem.* 2002; 234-235:177–184. [PubMed: 12162431]
- Castranova V. Signaling pathways controlling the production of inflammatory mediators in response to crystalline silica exposure: Role of reactive oxygen/nitrogen species. *Free Radic Biol Med.* 2004; 37:916–925. [PubMed: 15336307]
- Chen F, Castranova V, Shi X, Demers LM. New insights into the role of nuclear factor- κ B, a ubiquitous transcription factor in the initiation of diseases. *Clin Chem.* 1999a; 45:7–17. [PubMed: 9895331]
- Chen F, Demers LM, Vallyathan V, Lu Y, Castranova V, Shi X. Involvement of 5'-flanking κ B-like sites within bcl-x gene in silica-induced Bcl-x expression. *J Biol Chem.* 1999b; 274:35591–35595. [PubMed: 10585435]
- Cooper GS, Miller FW, Germolec DR. Occupational exposures and autoimmune diseases. *Int Immunopharmacol.* 2002; 2:303–313. [PubMed: 11811933]
- Ding M, Shi X, Lu Y, Huang C, Leonard S, Roberts J, Antonini J, Castranova V, Vallyathan V. Induction of activator protein-1 through reactive oxygen species by crystalline silica in JB6 cells. *J Biol Chem.* 2001; 276:9108–9114. [PubMed: 11096084]
- Fielden MR, Nie A, McMillian M, Elangbam CS, Trela BA, Yang Y, Dunn RT 2nd, Dragan Y, Fransson-Stehen R, Bogdanffy M, Adams SP, Foster WR, Chen SJ, Rossi P, Kasper P, Jacobson-Kram D, Tatsuoaka KS, Wier PJ, Gollub J, Halbert DN, Roter A, Young JK, Sina JF, Marlowe J, Martus HJ, Aubrecht J, Olaharski AJ, Roome N, Nioi P, Pardo I, Snyder R, Pery R, Lord P, Mattes W, Car BD, Predictive Safety Testing Consortium; Carcinogenicity Working Group. Interlaboratory evaluation of genomic signatures for predicting carcinogenicity in the rat. *Toxicol Sci.* 2008; 103:28–34. [PubMed: 18281259]
- Fubini B, Hubbard A. Reactive oxygen species (ROS) and reactive nitrogen species (RNS) generation by silica in inflammation and fibrosis. *Free Radic Biol Med.* 2003; 34:1507–1516. [PubMed: 12788471]
- Gentleman RC, Carey VJ, Bates DM, Bolstad B, Dettling M, Dudoit S, Ellis B, Gautier L, Ge Y, Gentry J, Hornik K, Hothorn T, Huber W, Iacus S, Irizarry R, Leisch F, Li C, Maechler M, Rossini AJ, Sawitzki G, Smith C, Smyth G, Tierney L, Yang JY, Zhang J. Bioconductor: Open software development for computational biology and bioinformatics. *Genome Biol.* 2004; 5:R80. [PubMed: 15461798]
- Ghaleb AM, Yang VW. The Pathobiology of Krüppel-like Factors in Colorectal Cancer. *Curr Colorectal Cancer Rep.* 2008; 4:59–64. [PubMed: 18504508]

- Hamadeh HK, Knight BL, Haugen AC, Sieber S, Amin RP, Bushel PR, Stoll R, Blanchard K, Jayadev S, Tennant RW, Cunningham ML, Afshari CA, Paules RS. Methapyrilene toxicity: Anchorage of pathologic observations to gene expression alterations. *Toxicol Pathol.* 2002; 30:470–482. [PubMed: 12187938]
- Hamilton RF Jr, Thakur SA, Holian A. Silica binding and toxicity in alveolar macrophages. *Free Radic Biol Med.* 2008; 44:1246–1258. [PubMed: 18226603]
- Hollander MC, Zhan Q, Bae I, Fornace AJ Jr. Mammalian GADD34, an apoptosis- and DNA damage-inducible gene. *J Biol Chem.* 1997; 272:13731–13737. [PubMed: 9153226]
- Hu S, Zhao H, Al-Humadi NH, Yin XJ, Ma JK. Silica-induced apoptosis in alveolar macrophages: Evidence of in vivo thiol depletion and the activation of mitochondrial pathway. *J Toxicol Environ Health Part A.* 2006; 69:1261–1284. [PubMed: 16754540]
- IARC. International Agency for Research on Cancer. Monograph on the evaluation of carcinogenic risk to human. 1997; 68:1–475.
- Ihaka R, Gentleman R. R: A language for data analysis and graphics. *J Comput Graphical Stat.* 1996; 5:299–314.
- Lang R, Hammer M, Mages J. DUSP meet immunology: Dual specificity MAPK phosphatases in control of the inflammatory response. *J Immunol.* 2006; 177:7497–7504. [PubMed: 17114416]
- Li R, Chen W, Yanes R, Lee S, Berliner JA. OKL38 is an oxidative stress response gene stimulated by oxidized phospholipids. *J Lipid Res.* 2007; 48:709–715. [PubMed: 17192422]
- Mao Y, Daniel LN, Whittaker N, Saffiotti U. DNA binding to crystalline silica characterized by Fourier-transform infrared spectroscopy. *Environ Health Perspect* 102 Suppl. 1994; 10:165–171.
- Mori A, Moser C, Lang SA, Hackl C, Gottfried E, Kreutz M, Schlitt HJ, Geissler EK, Stoeltzing O. Up-regulation of Krüppel-like factor 5 in pancreatic cancer is promoted by interleukin-1 β signaling and hypoxia-inducible factor-1 α . *Mol Cancer Res.* 2009; 7:1390–1398. [PubMed: 19671674]
- Mossman BT, Faux S, Janssen Y, Jimenez LA, Timblin C, Zanella C, Goldberg J, Walsh E, Barchowsky A, Driscoll K. Cell signaling pathways elicited by asbestos. *Environ Health Perspect* 105 Suppl. 1997; 5:1121–1125.
- Murray-Stewart T, Wang Y, Goodwin A, Hacker A, Meeker A, Casero RA Jr. Nuclear localization of human spermine oxidase isoforms - possible implications in drug response and disease etiology. *FEBS J.* 2008; 275:2795–2806. [PubMed: 18422650]
- Nakamura Y, Migita T, Hosoda F, Okada N, Gotoh M, Arai Y, Fukushima M, Ohki M, Miyata S, Takeuchi K, Imoto I, Katai H, Yamaguchi T, Inazawa J, Hirohashi S, Ishikawa Y, Shibata T. Krüppel-like factor 12 plays a significant role in poorly differentiated gastric cancer progression. *Int J Cancer.* 2009; 125:1859–1867. [PubMed: 19588488]
- Øvrevik J, Låg M, Schwarze P, Refsnes M. p38 and Src-ERK1/2 pathways regulate crystalline silica-induced chemokine release in pulmonary epithelial cells. *Toxicol Sci.* 2004; 81:480–490. [PubMed: 15240896]
- Porter DW, Ye J, Ma J, Barger M, Robinson VA, Ramsey D, McLaurin J, Khan A, Landsittel D, Teass A, Castranova V. Time course of pulmonary response of rats to inhalation of crystalline silica: NF- κ B activation, inflammation, cytokine production, and damage. *Inhal Toxicol.* 2002; 14:349–367. [PubMed: 12028809]
- Porter DW, Hubbs AF, Mercer R, Robinson VA, Ramsey D, McLaurin J, Khan A, Battelli L, Brumbaugh K, Teass A, Castranova V. Progression of lung inflammation and damage in rats after cessation of silica inhalation. *Toxicol Sci.* 2004; 79:370–380. [PubMed: 15056817]
- Robledo R, Mossman B. Cellular and molecular mechanisms of asbestos-induced fibrosis. *J Cell Physiol.* 1999; 180:158–166. [PubMed: 10395285]
- Santarelli L, Recchioni R, Moroni F, Marcheselli F, Governa M. Crystalline silica induces apoptosis in human endothelial cells in vitro. *Cell Biol Toxicol.* 2004; 20:97–108. [PubMed: 15242185]
- Sarkar D, Su ZZ, Lebedeva IV, Sauane M, Gopalkrishnan RV, Valerie K, Dent P, Fisher PB. mda-7 (IL-24) Mediates selective apoptosis in human melanoma cells by inducing the coordinated overexpression of the GADD family of genes by means of p38 MAPK. *Proc Natl Acad Sci USA.* 2002; 99:10054–10059. [PubMed: 12114539]

- Schlittenhardt D, Schober A, Strelau J, Bonaterra GA, Schmiedt W, Unsicker K, Metz J, Kinscherf R. Involvement of growth differentiation factor-15/macrophage inhibitory cytokine-1 (GDF-15/MIC-1) in oxLDL-induced apoptosis of human macrophages in vitro and in arteriosclerotic lesions. *Cell Tissue Res.* 2004; 318:325–333. [PubMed: 15459768]
- Sellamuthu R, Umbright C, Roberts JR, Chapman R, Young SH, Richardson D, Leonard H, McKinney W, Chen B, Frazer D, Li S, Kashon M, Joseph P. Blood gene expression profiling detects silica exposure and toxicity. *Toxicol Sci.* 2011; 122:253–264. [PubMed: 21602193]
- Stringer B, Kobzik L. Environmental particulate-mediated cytokine production in lung epithelial cells (A549): Role of preexisting inflammation and oxidant stress. *J Toxicol Environ Health Part A.* 1998; 55:31–44. [PubMed: 9747602]
- Thompson CA, Burcham PC. Protein alkylation, transcriptional responses and cytochrome c release during acrolein toxicity in A549 cells: Influence of nucleophilic culture media constituents. *Toxicol In Vitro.* 2008; 22:844–853. [PubMed: 18282682]
- Tong W, Harris S, Cao X, Fang H, Shi L, Sun H, Fuscoe J, Harris A, Hong H, Xie Q, Perkins R, Casciano D. Development of public toxicogenomics software for microarray data management and analysis. *Mutat Res.* 2004; 549:241–253. [PubMed: 15120974]
- Vallyathan V, Shi X. The role of oxygen free radicals in occupational and environmental lung diseases. *Environ Health Perspect* 105 Suppl. 1997; 1:165–177.
- Waring JF, Jolly RA, Ciurlionis R, Lum PY, Praestgaard JT, Morfitt DC, Buratto B, Roberts C, Schadt E, Ulrich RG. Clustering of hepatotoxins based on mechanism of toxicity using gene expression profiles. *Toxicol Appl Pharmacol.* 2001; 175:28–42. [PubMed: 11509024]
- Yu J, Baron V, Mercola D, Mustelin T, Adamson ED. A network of p73, p53 and Egr1 is required for efficient apoptosis in tumor cells. *Cell Death Differ.* 2007; 14:436–446. [PubMed: 16990849]

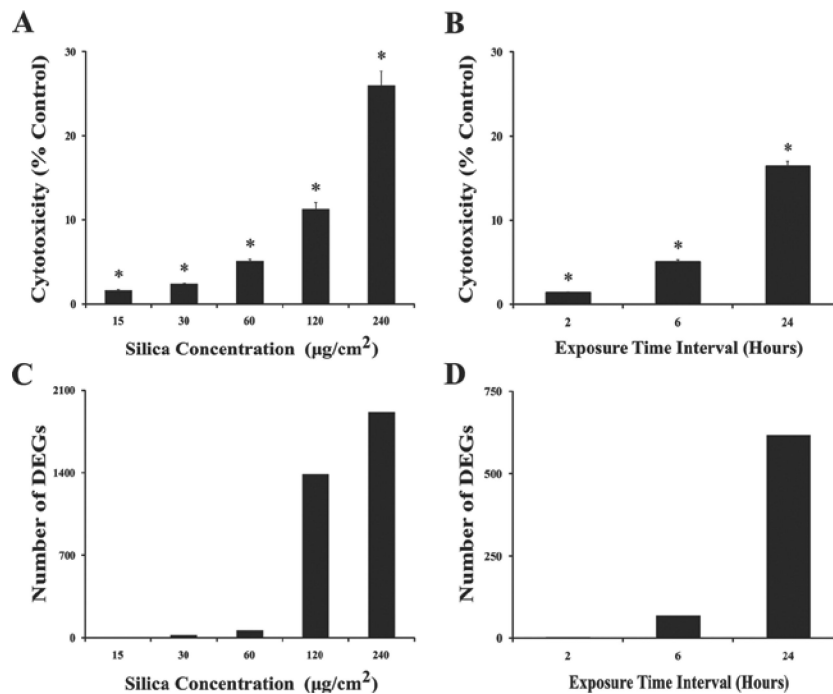


Figure 1. Cytotoxicity and differential gene expression profile in silica exposed A549 cells. Exponentially growing A549 cells were treated with crystalline silica particles at concentrations of 15, 30, 60, 120, and 240 $\mu\text{g}/\text{cm}^2$ for 6-hours (A and C) or 60 $\mu\text{g}/\text{cm}^2$ for time intervals of 2-, 6-, or 24-hours (B and D). Cytotoxicity and global gene expression profile were determined by LDH assay and microarray analysis, respectively, as described in the Materials and methods section. Cytotoxicity and the number of differentially expressed genes (DEGs) (FDR p value < 0.05) were calculated with respect to the corresponding control. *Statistically significant, $p < 0.05$ ($n = 5$).

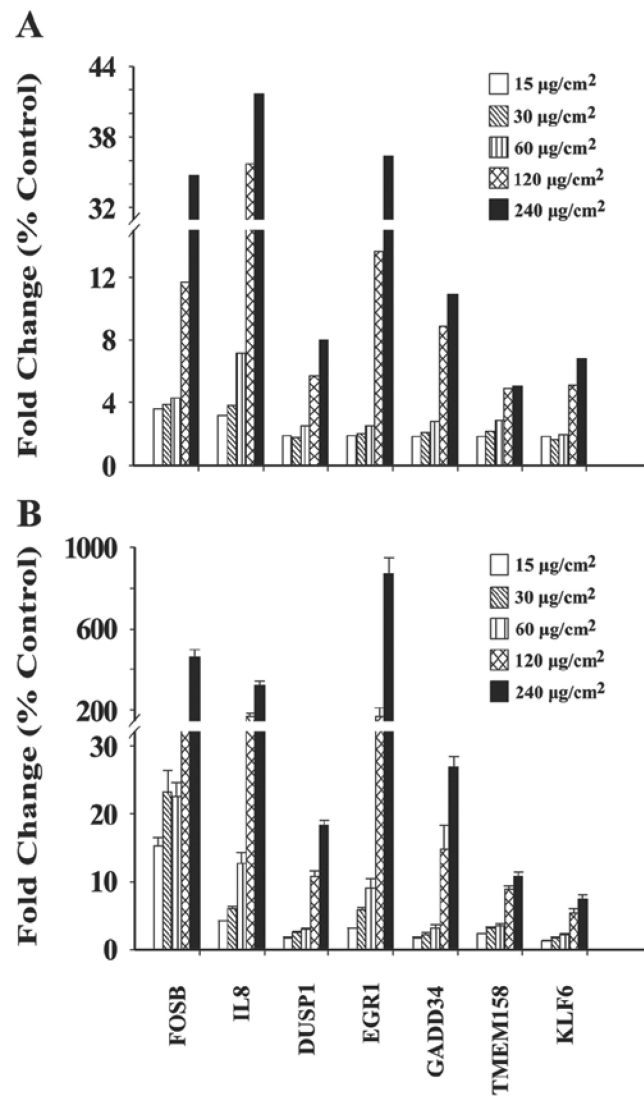


Figure 2.

Validation of microarray results by QRT-PCR. A set of seven genes which were overexpressed in the silica exposed A549 cells as evidenced from the microarray data were analyzed by QRT-PCR as described in the Materials and methods section. Data presented is the mean (A) or mean \pm SE (B) fold-change ($n = 5$) in the silica exposed cells compared with the corresponding control cells. The genes represented in A are in the same order as in B and, therefore, the x-axis is labeled only in B. All genes, with the exception of *KLF6* at the lowest silica concentration ($15 \mu\text{g}/\text{cm}^2$) were significantly ($p < 0.05$) differentially expressed compared with the corresponding controls. (A). Microarray results, and (B). QRT-PCR results.

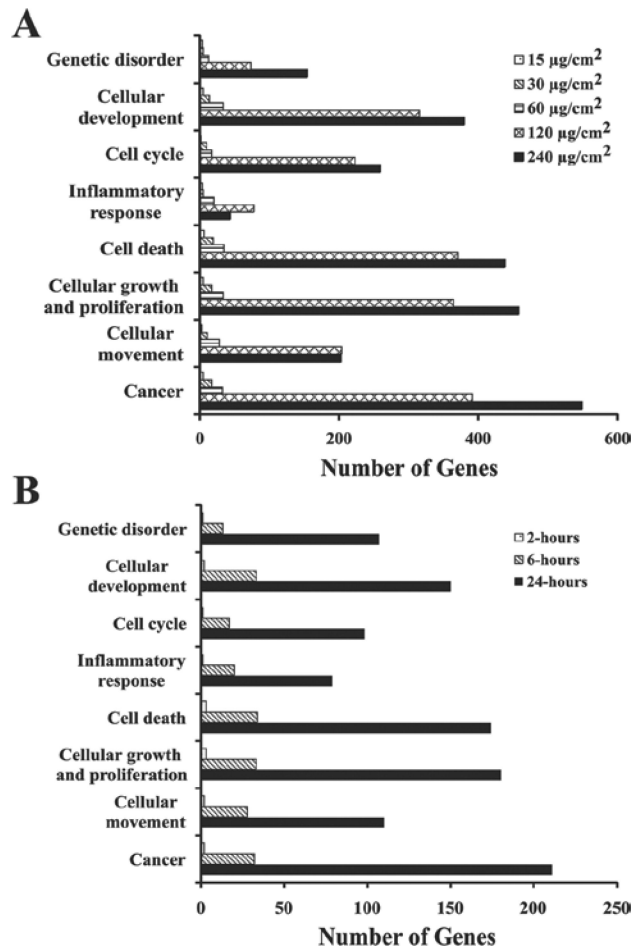


Figure 3. Effect of silica concentration and duration of exposure on the major biological functions perturbed by silica exposure in A549 cells. The number of genes involved in the top eight ranking biological processes perturbed by silica exposure as identified by IPA analysis of the significantly differentially expressed genes in the A549 cells are presented. Data represents the mean of five independent experiments. (A). Effect of silica concentration; (B). Effect of silica exposure duration.

Table 1

Nucleotide sequences of primers of the genes selected for QRT-PCR analysis.

Gene Symbol	GenBank Number	Forward Primer (5'-3')	Reverse Primer (3'-5')
<i>FOSB</i>	NM 006732	TCCTCCGCCTGTGTCCATCTG	GTCAGACGACAGCTGGAGCATTG
<i>DUSP1</i>	NM 004419	ACCAGGCTTGCAAATGAACTTCAG	ACATGCTGTGCTCCCCTAATGG
<i>EGR1</i>	NM 001964	AGATGGAGGTTCTCAGAGCCAAGTC	GGAAGTGGGCAGAAAGGATTGTTG
<i>GADD34</i>	NM 014330	ACAGGATCAGCCGAGGATGAAAG	ACACCCAGGCCTTCAAGAAAGC
<i>TMEM158</i>	NM 015444	GTTTGTGCTGCGCTTCCAGTTC	CCATTTCCCTCCTCTCCGTCTTC
<i>KLF6</i>	NM 001300	CGGTTTGATCTTCCATTGCTCAAG	GTGGCAGGAAACACTCAAGTTTG
<i>IL8</i>	NM 000584	TGTTCCACTGTGCCTTGTTTCTC	TGCTTCCACATGTCTCACAACATC
<i>B2M</i>	NM 004048	TGCTGTCTCCATGTTGATGTATCT	TCTCTGCTCCCCACCTCTAAGT

Author Manuscript

Author Manuscript

Author Manuscript

Author Manuscript

Table 2

Top biological functions generated by analyzing the significantly differentially expressed genes by IPA in the A549 cells and rat lungs exposed to crystalline silica.

Biological Function	A549 cells		Rat lungs	
	Rank *	Number of molecules **	Rank *	Number of molecules **
Cancer	1	211	1	670
Cellular movement	2	110	2	405
Cellular growth and proliferation	3	180	3	634
Cell death	4	174	9	583
Inflammatory response	5	79	8	361
Cell cycle	6	98	57	254
Cellular development	7	150	13	451
Genetic disorder	8	107	15	164
Antigen presentation	9	27	12	108
Cell-to-cell interaction and communication	10	101	4	369

In general, the biological functions affected by silica exposure, as identified by IPA analysis, in the A549 cells treated with silica at various concentrations (15, 30, 60, 120 and 240 $\mu\text{g}/\text{cm}^2$) and exposure durations (60 $\mu\text{g}/\text{cm}^2$ for 2-, 6-, and 24-hours) were similar. Data obtained from the A549 cells treated with silica at the final concentration of 60 $\mu\text{g}/\text{cm}^2$ for 24-hours is presented as the representative.

* Approximately 75 biological function categories were considered for ranking and the ranking was based on the IPA *p* value of the biological function category.

** Number of molecules represents the number of differentially expressed genes in the silica exposed A549 cells and rat lungs belonging to the corresponding biological function category.

Table 3

Differentially expressed genes in A549 cells exposed to crystalline silica.

Gene		Crystalline silica ($\mu\text{g}/\text{cm}^2$)					Time interval (hrs)		
		15	30	60	120	240	2	6	24
Reactive Oxygen Species									
<i>SOD2</i>	<i>Superoxide dismutase 2</i>	1.08	1.11	1.21 *	1.98 *	2.50 *	-1.05	1.21 *	4.52 *
<i>CAT</i>	<i>Catalase</i>	1.02	-1.05	-1.07	-1.16 *	-1.14 *	-1.08	-1.07	-1.24
<i>SMOX</i>	<i>Spermine oxidase</i>	1.33	1.39 *	1.55 *	2.99 *	3.52 *	1.33	1.55 *	2.55 *
<i>CYR61</i>	<i>Cysteine-rich angiogenic inducer 61</i>	1.12	1.59 *	1.90 *	2.47 *	1.57 *	2.11 *	1.90 *	1.55 *
Antioxidant/Oxidative Stress									
<i>NFE2L2</i>	<i>Nuclear factor erythroid derived 2 like 2</i>	1.03	1.05	1.15	1.83 *	1.61 *	1.28 *	1.15	-1.05
<i>NFκB1</i>	<i>Nuclear factor of κ light polypeptide gene enhancer in B-cells 1</i>	-1.04	1.18	1.31 *	2.00 *	2.03 *	1.11	1.31 *	1.50 *
<i>NFκB2</i>	<i>Nuclear factor of κ light polypeptide gene enhancer in B-cells 2</i>	1.04	1.02	1.05	1.12 *	1.11 *	1.05	1.05	1.09 *
<i>NFκBIZ</i>	<i>Nuclear factor of κ light polypeptide gene enhancer in B-cells inhibitor, ζ</i>	1.15	1.21	1.23	2.51 *	3.31 *	1.18	1.23	2.86 *
<i>DUSP1</i>	<i>Dual specificity phosphatase 1</i>	1.24	1.22 *	1.49 *	2.47 *	3.00 *	1.56	1.49 *	1.55 *
<i>DUSP5</i>	<i>Dual specificity phosphatase 5</i>	1.92 *	1.79 *	2.48 *	5.74 *	8.02 *	2.84 *	2.48 *	2.98 *
<i>FOS</i>	<i>v-fos FBJ murine osteosarcoma viral oncogene homolog</i>	1.24	1.36	1.42	3.93 *	20.34 *	2.06 *	1.42	1.24 *
<i>junb</i>	<i>jun B proto-oncogene</i>	1.02	-1.00	1.07	1.46 *	1.72 *	1.20	1.07	-1.03
<i>c-JUN</i>	<i>jun oncogene</i>	1.27	1.46	1.87 *	5.46 *	10.64 *	2.17 *	1.87 *	2.40 *
<i>STC1</i>	<i>Stanniocalcin 1</i>	1.63 *	1.75 *	2.37 *	4.67 *	5.40 *	1.90 *	2.37 *	2.75 *
<i>STC2</i>	<i>Stanniocalcin 2</i>	1.22	1.31 *	1.55 *	2.06 *	2.03 *	1.02	1.55 *	3.35 *
Inflammation									
<i>IRF1</i>	<i>Interferon regulatory factor 1</i>	1.10	1.06	1.14	1.54 *	1.33 *	-1.04	1.54 *	1.15
<i>RELA</i>	<i>v-rel reticuloendotheliosis viral oncogene homolog A</i>	1.02	1.06	1.11 *	1.22 *	1.12 *	1.05	1.11 *	1.13 *
<i>relb</i>	<i>v-rel reticuloendotheliosis viral oncogene homolog B</i>	1.20 *	1.24 *	1.51 *	1.92 *	1.73 *	-1.01	1.51 *	1.92 *
<i>IL1A</i>	<i>Interleukin 1 α</i>	1.05	1.02	1.05	1.86 *	2.62 *	ND	1.05	1.22 *
<i>IL1B</i>	<i>Interleukin 1 β</i>	ND	-1.00	1.02	1.28 *	1.45 *	ND	1.28 *	1.6 *
<i>IL6</i>	<i>Interleukin 6</i>	1.12	1.24	1.58 *	6.17 *	8.51 *	1.43 *	1.58 *	6.14 *
<i>IL8</i>	<i>Interleukin 8</i>	3.16 *	3.84 *	7.13 *	35.72 *	41.60 *	9.77 *	7.13 *	18.21 *
<i>IL11</i>	<i>Interleukin 11</i>	1.08	1.23	1.47	3.75 *	4.92 *	1.89 *	1.47	1.49 *
<i>IRAK2</i>	<i>Interleukin-1 receptor-associated kinase 2</i>	1.63 *	1.77 *	1.89 *	5.56 *	7.15 *	1.66 *	1.89 *	3.54 *
<i>PTGS2</i>	<i>Prostaglandin-endoperoxide synthase 2</i>	1.51	1.55 *	2.21 *	11.13 *	15.09 *	2.38 *	2.21 *	3.91 *

Gene	Crystalline silica ($\mu\text{g}/\text{cm}^2$)					Time interval (hrs)			
	15	30	60	120	240	2	6	24	
<i>CCL2/MCP1</i>	Chemokine (C-C motif) ligand 2	1.68	1.77*	1.67*	3.30*	3.57*	1.38	1.67*	3.23*
<i>CL20/MIP3α</i>	Chemokine (C-C motif) ligand 20	1.06	1.06	1.23*	3.20*	4.16*	1.13	1.23*	2.39*
<i>CXCL1/GRO1</i>	Chemokine (C-X-C motif) ligand 1	ND	-1.00	1.04	1.41*	1.50*	ND	1.04	1.60*
<i>CXCL2/MIP-2</i>	Chemokine (C-X-C motif) ligand 2	1.24	1.12	1.29	3.81*	3.58*	1.38	1.29	3.23*
<i>CXCL5</i>	Chemokine (C-X-C motif) ligand 5	1.24	1.17	1.57*	2.70*	4.16*	1.13	1.57*	2.39*
<i>CXC18/IL8</i>	Interleukin 8	3.16*	3.84*	7.13*	35.72*	41.60*	9.77*	7.13*	18.21*
<i>PLAU</i>	Plasminogen activator urokinase	1.23	1.44	1.75*	2.44*	1.83*	1.48*	1.75*	1.53*
<i>ITGA2</i>	Integrin α 2 (CD49B, α 2 subunit of VLA-2 receptor)	-1.05	1.11	1.26	1.74*	1.57*	1.03	1.26	1.81*
<i>MMP10</i>	Matrix metalloproteinase 10	ND	1.03	1.04	1.87*	3.82*	ND	1.04	1.71*
<i>CEBPB</i>	CCAAT/enhancer binding protein	1.13	1.23*	1.42*	2.78*	3.62*	1.86*	1.42*	2.08*
Apoptosis									
<i>NFE2L2</i>	Nuclear factor erythroid derived 2 like 2	1.03	1.05	1.15	1.83*	1.61*	1.28*	1.15	-1.05
<i>NFκB1</i>	Nuclear factor of κ light polypeptide gene enhancer in B-cells 1	-1.04	1.18	1.31*	2.00*	2.03*	1.11	1.31*	1.50*
<i>NFκB2</i>	Nuclear factor of κ light polypeptide gene enhancer in B-cells 2 (p49/p100)	1.04	1.02	1.05	1.12*	1.11*	1.05	1.05	1.09*
<i>NFκBIA</i>	Nuclear factor of κ light polypeptide gene enhancer in B-cells inhibitor α	1.10	1.32*	1.45*	2.93*	4.48*	1.35	1.45*	1.94*
<i>NFκBIZ</i>	Nuclear factor of κ light polypeptide gene enhancer in B-cells inhibitor, ζ	1.15	1.21	1.23	2.51*	3.31*	1.18	1.23	2.86*
<i>GDF-15</i>	Growth differentiation factor 15	1.65*	1.50*	1.75*	5.33*	9.68*	1.74	1.75*	2.38*
<i>GADD45α</i>	Growth arrest and DNA-damage-inducible 45 α	1.19	1.46*	1.62*	3.08*	3.81*	1.59*	1.62*	1.79*
<i>GADD34</i>	Growth arrest and DNA-damage-inducible 34	1.86*	2.10*	2.82*	5.88*	10.93*	2.72*	2.82*	3.56*
<i>EGR1</i>	Early Growth Response 1	1.91*	2.05*	2.51*	13.65*	36.34*	6.46*	2.51*	2.49*
<i>BIRC3</i>	Baculoviral IAP repeat-containing 3	1.27	1.58*	2.01*	5.78*	8.51*	1.59*	2.01*	2.43*
<i>c-FOS</i>	v-fos FBJ murine osteosarcoma viral oncogene homolog	1.24	1.36	1.42	3.93*	20.34*	2.06*	1.42	1.24*
<i>FOSB</i>	FBJ murine osteosarcoma viral oncogene homolog B	3.58*	3.87*	4.30*	11.64*	34.73*	9.83*	4.30*	3.74*
<i>FOSL1</i>	FOS-like antigen 1	1.10	1.31*	1.63*	2.93*	2.33*	1.39*	1.63*	1.44*
<i>CYR61</i>	Cysteine-rich angiogenic inducer 61	1.12	1.59*	1.90*	2.47*	1.57*	2.11*	1.90*	1.55*
<i>JUND</i>	jun D proto-oncogene	-1.03	1.10	1.20	2.26*	3.26*	1.17	1.20	-1.01
<i>OKL-38</i>	Pregnancy-induced growth inhibitor	-1.18	1.10	1.16	1.79*	2.49*	1.32	1.16	-1.16
Cancer									
<i>EFNA1</i>	Ephrin-A1	1.31	1.32	1.45	2.72*	2.93*	1.10	1.45	1.88*
<i>MYC</i>	v-myc myelocytomatosis viral oncogene homolog (avian)	1.14	1.22	1.32	1.69*	2.16*	1.23	1.32	1.16

Gene		Crystalline silica ($\mu\text{g}/\text{cm}^2$)					Time interval (hrs)		
		15	30	60	120	240	2	6	24
<i>CEBPB</i>	<i>CCAAT/enhancer binding protein</i>	1.13	1.23*	1.42*	2.78*	3.62*	1.86*	1.42*	2.08*
<i>TRIB1</i>	<i>Tribbles homolog 1 (Drosophila)</i>	1.13	1.09	1.22	2.57*	3.90*	1.34	1.22	1.55*
<i>PTGS2</i>	<i>Prostaglandin-endoperoxide synthase 2</i>	1.51	1.55*	2.21*	11.13*	15.09*	2.38*	2.21*	3.91*
<i>ZFP36</i>	<i>Zinc finger protein 36</i>	1.36	1.44	1.58*	6.43*	10.65*	2.16*	1.58*	1.10
<i>KLF2</i>	<i>Kruppel-like factor 2</i>	1.33	1.67	1.87*	2.38*	1.90*	1.88*	1.87*	1.18*
<i>KLF6</i>	<i>Kruppel-like factor 6</i>	1.38*	1.61*	1.97*	5.14*	6.84*	2.03*	1.97*	2.38*
<i>KLF11</i>	<i>Kruppel-like factor 11</i>	1.08	1.13	1.21	1.60*	1.65*	1.14	1.21	1.58*
<i>KLF13</i>	<i>Kruppel-like factor 13</i>	1.14	1.22	1.38*	1.71*	1.32*	1.01	1.38*	1.15
<i>ETS1</i>	<i>v-ets erythroblastosis virus E26 oncogene homolog 1</i>	1.36	1.44*	1.77*	3.50*	3.58*	1.35*	1.77*	2.06*
<i>DDIT3</i>	<i>DNA-damage-inducible transcript 3</i>	1.36*	1.48*	1.63*	3.11*	4.15*	1.25	1.63*	2.17*
<i>FGF2</i>	<i>Fibroblast growth factor 2</i>	1.00	1.00	1.10	1.25*	1.27*	1.07	1.10	1.07
Cellular Growth and Proliferation									
<i>EGR1</i>	<i>Early Growth Response 1</i>	1.91*	2.05*	2.51*	13.65*	36.34*	6.46*	2.51*	2.49*
<i>RELB</i>	<i>v-rel reticuloendotheliosis viral oncogene homolog B</i>	1.20*	1.24*	1.51*	1.92*	1.73*	-1.01	1.51*	1.92*
<i>IL8</i>	<i>Interleukin 8</i>	3.16*	3.84*	7.13*	35.72*	41.60*	9.77*	7.13*	18.21*
<i>DUSP5</i>	<i>Dual specificity phosphatases 5</i>	1.92*	1.79*	2.48*	5.74*	8.02*	2.84*	2.48*	2.98*
<i>FST</i>	<i>Follistatin</i>	1.41*	1.62*	2.20*	4.57*	4.60*	1.25	2.20*	2.48*
<i>ETS1</i>	<i>v-ets erythroblastosis virus E26 oncogene homolog 1</i>	1.36	1.44*	1.77*	3.50*	3.58*	1.35*	1.77*	2.06*
Cell Cycle									
<i>EGR1</i>	<i>Early Growth Response 1</i>	1.91*	2.05*	2.51*	13.65*	36.34*	6.46*	2.51*	2.49*
<i>ETS1</i>	<i>v-ets erythroblastosis virus E26 oncogene homolog 1</i>	1.36	1.44*	1.77*	3.50*	3.58*	1.35*	1.77*	2.06*
<i>STC1</i>	<i>Stanniocalcin 1</i>	1.63*	1.75*	2.37*	4.67*	5.40*	1.90*	2.37*	2.75*
<i>c-JUN</i>	<i>jun oncogene</i>	1.27	1.46	1.87*	5.46*	10.64*	2.17*	1.87*	2.40*
<i>NFκBIA</i>	<i>Nuclear factor of κ light polypeptide gene enhancer in B-cells inhibitor α</i>	1.10	1.32*	1.45*	2.93*	4.48*	1.35	1.45*	1.94*
<i>PTGS2</i>	<i>Prostaglandin-endoperoxide synthase 2</i>	1.51	1.55*	2.21*	11.13*	15.09*	2.38*	2.21*	3.91*
Cellular Development									
<i>CSF2</i>	<i>Colony stimulating factor 2 (granulocyte-macrophage)</i>	ND	1.07	1.13	2.48*	3.81*	1.08	1.13	2.04*
<i>CEBPB</i>	<i>CCAAT/enhancer binding protein (C/EBP)</i>	1.13	1.23*	1.42*	2.78*	3.62*	1.86*	1.42*	2.08*
<i>EGR1</i>	<i>Early Growth Response 1</i>	1.91*	2.05*	2.51*	13.65*	36.34*	6.46*	2.51*	2.49*
<i>FOSL1</i>	<i>FOS-like antigen 1</i>	1.10	1.31*	1.63*	2.93*	2.33*	1.39*	1.63*	1.44*
<i>c-JUN</i>	<i>jun oncogene</i>	1.27	1.46	1.87*	5.46*	10.64*	2.17*	1.87*	2.40*

Gene		Crystalline silica ($\mu\text{g}/\text{cm}^2$)					Time interval (hrs)		
		15	30	60	120	240	2	6	24
<i>FOXO1</i>	<i>Forkhead box O1</i>	1.17	1.21 *	1.41 *	2.06 *	1.76 *	1.16	1.41 *	1.33 *

Data represent the fold change in expression of the individual genes and are mean of five independent microarray experiments.

Some of the genes are listed under multiple categories since they are involved in multiple functions.

ND, Gene expression not detected.

* Statistically significant change in expression compared to the corresponding control (FDR p value < 0.05).

Author Manuscript

Author Manuscript

Author Manuscript

Author Manuscript